AN INVESTIGATION OF THE PERFORMANCE OF SHARP EDGED JET ENGINE INLETS AT ZERO FORWARD VELOCITY

by

LEROY LAWRENCE PRESLEY

A THESIS

submitted to

OREGON STATE COLLEGE

in partial fulfillment of
the requirements for the
degree of

MASTER OF SCIENCE

June 1956

APPROVED:

Redacted for Privacy

Assistant Professor of Aeronautical Engineering

In Charge of Major

Redacted for Privacy

Chairman of Department of Mechanical Engineering

Redacted for Privacy

Chairman of School Graduate Committee

Redacted for Privacy

Dean of Graduate School

Date thesis is presented May 10, 1956

Typed by Janet de Laubenfels

TABLE OF CONTENTS

LIST OF FIGURES

LIST OF FIGURES (CONTINUED)

ACKNOWLEDGEMENT

The author wishes to express his appreciation for the advice and aid received from Assistant Professor Harm Buning of the Department of Mechanical Engineering. He also wishes to thank the entire mechanical engineering staff for their aid and support.

To the Shell Oil Company, the author extends his most heartfelt thanks for their aid.

AN INVESTIGATION OF THE PERFORMANCE OF SHARP EDGED JET ENGINE INLETS AT ZERO FORWARD VELOCITY

INTRODUCTION

General

The turbojet engine is one of the most widely used power plants in the aircraft industry at the present time. As the era of high speed flight advances, this type of propulsive unit will become more and more predominant. The turbojet engine, however, requires a large mass flow of air in order to derive its thrust. This mass of air, in order to reach the jet engine, must pass through some sort of intake system, defined here as the portion of the propulsive unit connecting the front of the compressor to the free stream atmosphere. This thesis is concerned with an investigation of some of the problems encountered in such an air intake system.

Before the problems investigated in this thesis can be defined, it is necessary to have some knowledge of the role of the inlet in the overall cycle of the propulsive unit. The turbojet propulsive unit can be represented schematically as shown in figure 1.

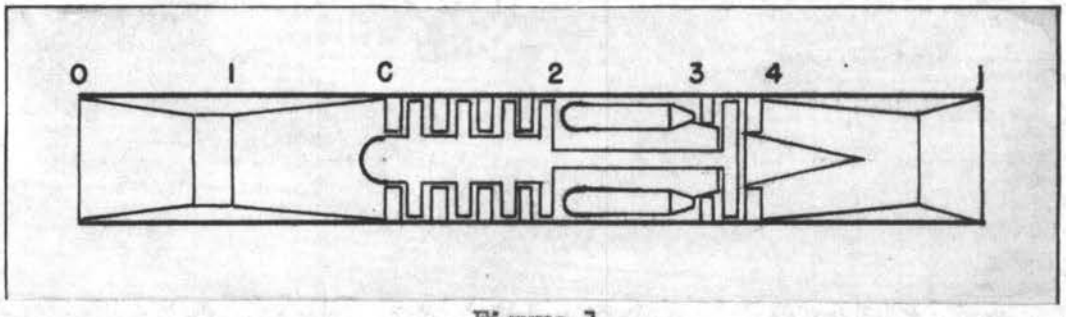

Figure 1

Schematic Diagram of Turbojet Propulsive Unit

The individual components are as listed below:

o-c inlet

c-2 compressor

2-3 combustion chamber

3-4 turbine

4-j jet nozzle

If an ideal cycle is considered, the processes occurring in a turbojet propulsive unit can be represented best on an enthalpy-entropy diagram. Such a cycle is qualitatively shown in figure 2.

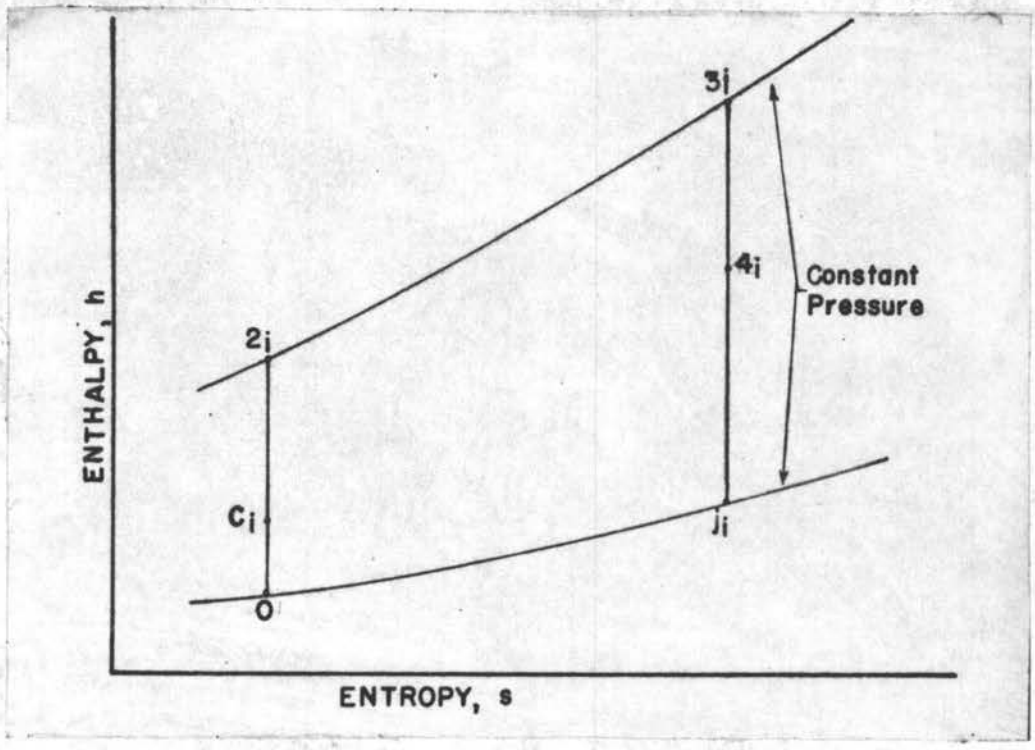

Figure 2

Enthalpy-Entropy Diagram

The individual processes that occur in an ideal cycle are:

o-c The air is diffused isentropically from the pressure at point o to that at c.

c-2 The air is compressed isentropically from the pressure at c to that at 2.

2-3 Heat is added to the air at constant pressure.

3-4 Energy is extracted isentropically to power the compressor.

4-j The air expands isentropically to atmospheric pressure.

On an enthalpy-entropy diagram, the constant pressure lines are divergent, therefore enabling more work to be obtained from the cycle than was put into it. The output of the cycle is the difference in enthalpy from point 3 to j, while the input into the cycle is the change in enthalpy from point 2 to o. The difference between the input and the output can be defined as the thrust of the unit. In equation form, this thrust would be:

$$T_i = (h_{3i} - h_{ji}) - (H_{2i} - h_o)$$

If a cycle is now considered in which the inlet process is non-ideal, while holding the remainder of the cycle ideal, the effect upon the thrust would be as represented on the enthalpy-entropy diagram of figure 3.

In considering the inlet process to be non-ideal, the result is that the total pressure at C is less than in the ideal cycle. The compression ratio of the compressor is fixed for any given operating condition; thus, the combustion would take place at a lower pressure, but would still reach the same temperature. Due to the divergence of the constant pressure lines, it is seen that the ideal work from the cycle is greater than the actual work from the cycle, while the work input is the same for both cases. This means that the actual thrust

would be:

$$T = (h_{3a}-h_{ja}) - (h_{2i}-h_o)$$

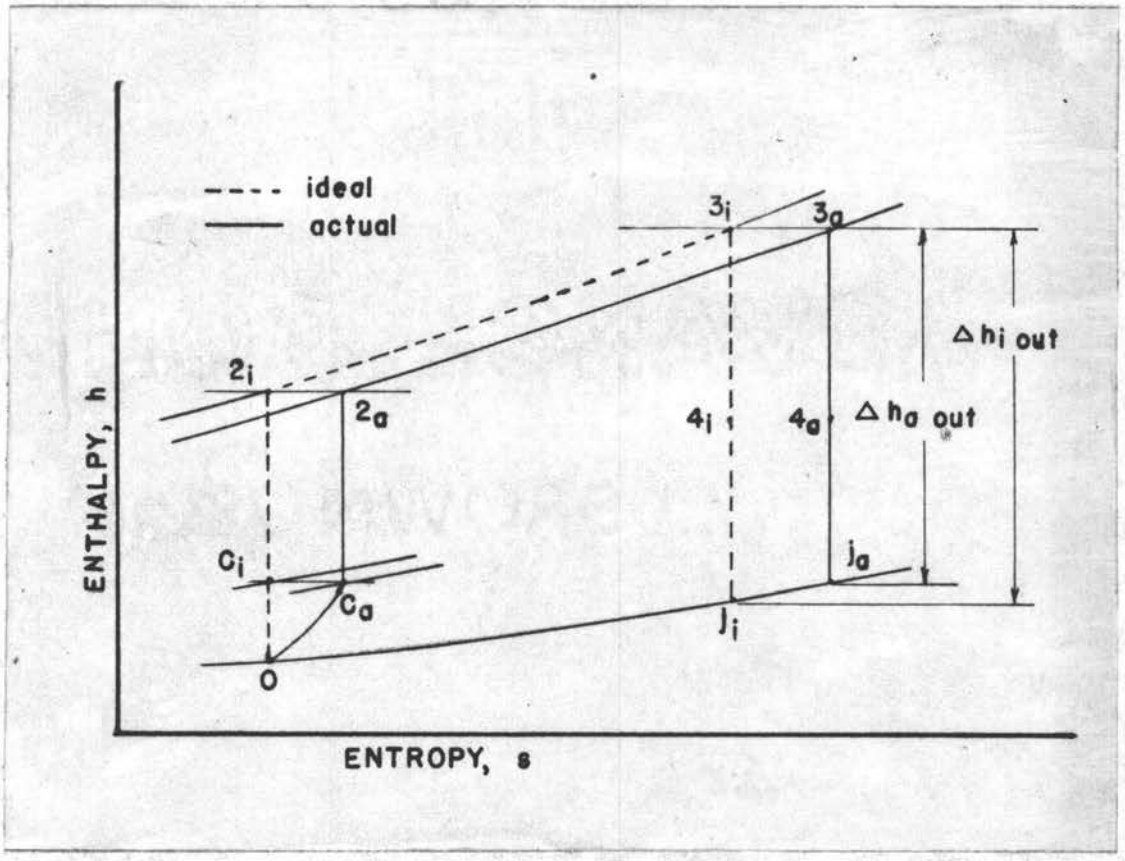

Figure 3

Enthalpy-Entropy Diagram

One of the major problems of inlet design is to design the inlet to fit any given range of variables, yet be able to obtain, over the entire range, near isentropic pressure recovery at the compressor entrance. In the solution of this problem, many and varied configurations have been developed. These can be divided into two distinct classifications, namely those for subsonic flight and those for supersonic flight.

Subsonic inlets are characterized by thick leading edges, so called lips, which fair immediately into diverging sections. The thickness of the lips is inversely proportional to the design velocity; for example, the slower the velocity, the thicker the lip. The major problems of subsonic inlets have been solved and the operating characteristics over a broad range of conditions have been defined.

The design of supersonic inlets to meet the entire range of conditions is not as simple as for the subsonic case. The air that enters the inlet is travelling supersonically and it must be: (1) first slowed down, (2) then changed from supersonic to subsonic, (3) and then diffused in a diverging section to the entrance of the compressor.

The machinery for performing the operations of a supersonic inlet and reasons for doing so are:

(1) The air is slowed down, reducing the Mach number, by means of either a series of shock waves, a converging channel, or both. The shock waves are usually generated by small angles so as to minimize the total pressure loss associated with them. The converging channel also aids in reducing the Mach number due to the change in area from point to point.

(2) The air is changed from supersonic to subsonic by passing through a normal shock wave. It is desirable to have the air preceding the normal shock as near as possible to $M = 1$ in order to minimize the total pressure loss across it.

(3) The air is then diffused subsonically in the divergent section aft of the most rearward point of minumum area.

Supersonic inlets have sharp edged lips and are designed to obtain optimum efficiency over some supersonic Mach number range. These sharp edges have the inherent disadvantage of being very inefficient at subsonic speeds, and especially so for static conditions. The result is a large loss in total pressure at the entrance to the compressor. This pressure loss may be as high as 20% H_o for maximum mass flow and results in a considerable loss in the static thrust of the propulsive unit.

Object.

The object of this thesis is to discuss the results of an investigation of the performance of sharp edged jet engine inlets at zero forward velocity. The following design parameters will be considered in order to determine their effect upon the performance of such inlets:

(1) The effect of contraction ratio--A_1/A_o.

(2) The effect of internal wall curvature.

(3) The effect of boundary layer control in the immediate region of the lips.

The effect of these parameters will be investigated in the light of improving the static performance, yet not rendering the inlet unsatisfactory for supersonic performance.

NOTATION

The following symbols and subscripts are used throughout this thesis:

A	Area
M	Mach number local velocity/local speed of sound
p	Static pressure
H	Total pressure
d	Diameter
m	Mass flow
y	Ordinate normal to the axis of the body
x	Ordinate parallel to the axis of the body
γ	Ratio of the specific heats
ρ	Density of the air
m_*	Mass flow to establish critical flow in the minimum area section
h	Enthalpy
s	Entropy
T	Thrust
t	Temperature

Subscripts

o	Free stream conditions
1	Point of most rearward minimum area in the inlet
c	Simulated compressor entrance
2	Entrance to the combustion chambers
3	Entrance to the turbine
4	Entrance to the jet nozzle

j	Outlet of the jet nozzle
i	Ideal process
a	Actual process

DESCRIPTION OF MODEL, INSTRUMENTATION AND TESTS

Design of Model

In the design of the model, the ratios used would correspond to a composite of the turbojet engines in use at the present time. The ratio of the diameters at the front of the jet engine, D_b/D_c, was 0.45. The diameter D_b is the diameter of the boss or hub housing auxillary components, and D_c is the diameter to the tip of the compressor blades. These diameters are shown schematically in figure 4. The ratio of the area of the entrance of the inlet to the area of the entrance to the compressor, A_o/A_c was unity.

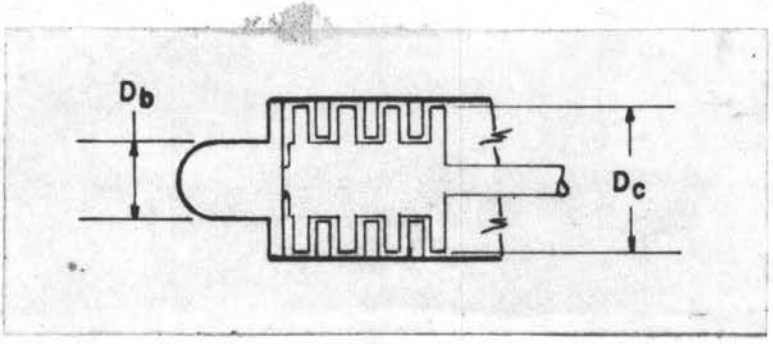

Figure 4

Front of Typical Jet Engine

The parameters used in the design of the inlets were:

(1) All internal angles were held small, in the order of 5° so as to be acceptable for supersonic flight.

(2) For those inlets having contraction ratio, A_1 smaller than A_o, it was to be held constant. It was to be sufficient to provide isentropic diffusion at M = 2.0.

(3) The minimum area was to be held constant for all of the inlets.

(4) The length of all of the inlets was to be the same.

Using these design parameters, the inlets that resulted are shown in figures 5 and 6. Each of these inlets was different for the reasons discussed in the following paragraphs.

Inlet 1. This inlet had elliptical lips and was designed to provide a norm for the performance of the other inlets. The contraction ratio, A_1/A_o, of this inlet was 0.638. This would give isentropic diffusion at M_o= 1.98, allowing 5% reduction in area for boundary layer growth.

Inlet 2. The dimensions of this inlet were the same as those for inlet one, except that the lips were sharp. The internal contour was of a straight conical section. This inlet was designed to show the effect of contraction ratio upon the performance of sharp edged inlets.

Inlet 3. The shape and dimensions of this inlet were the same as those for inlet number two, except that the internal walls were slightly curved. The initial angle of the lip was 7° and the wall was faired into the minimum area section. This inlet was designed to show the effect of internal wall curvature upon the performance of sharp edged inlets.

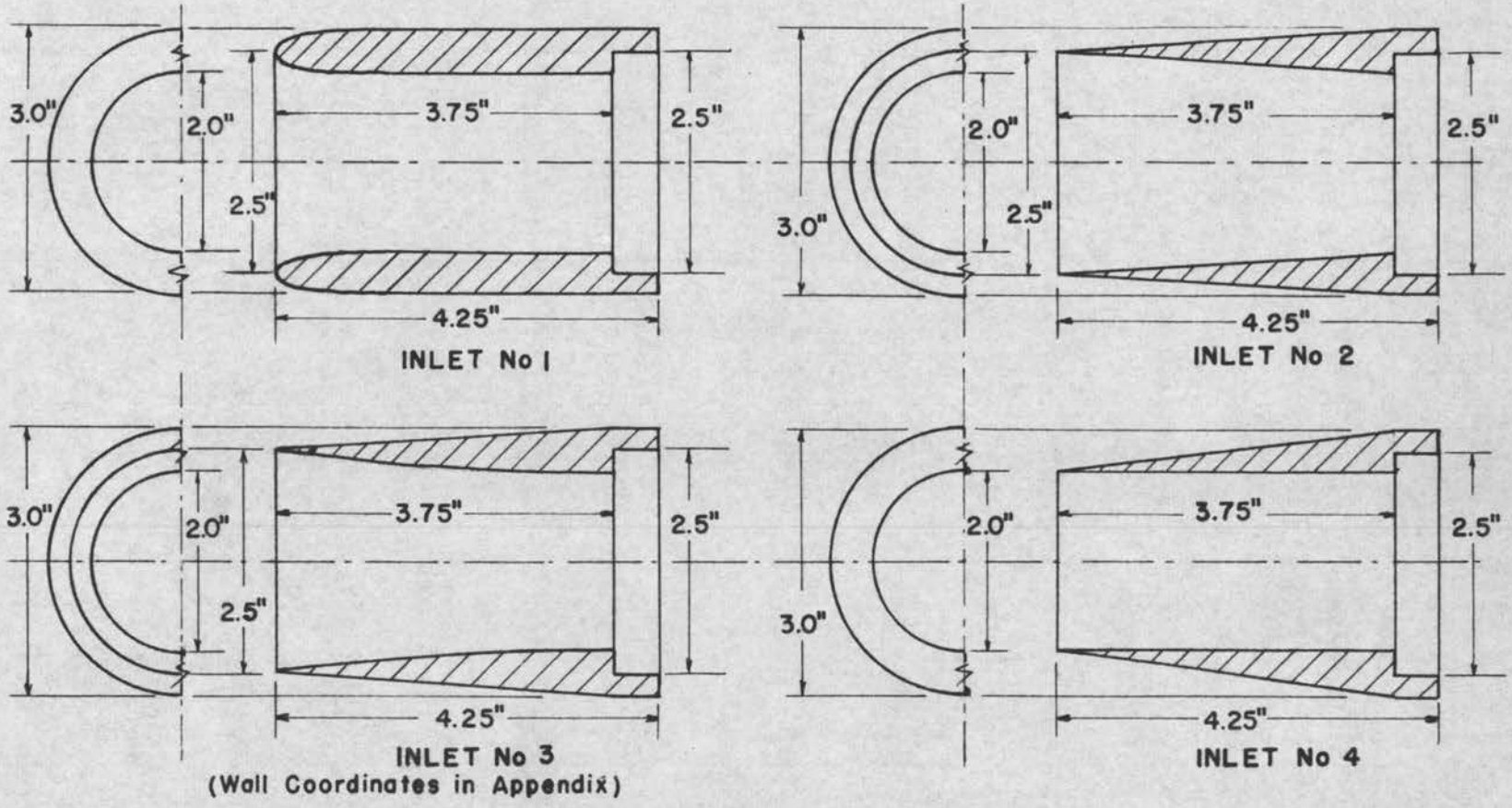

FIG. 5

DETAILS OF THE FOUR BASIC INLETS

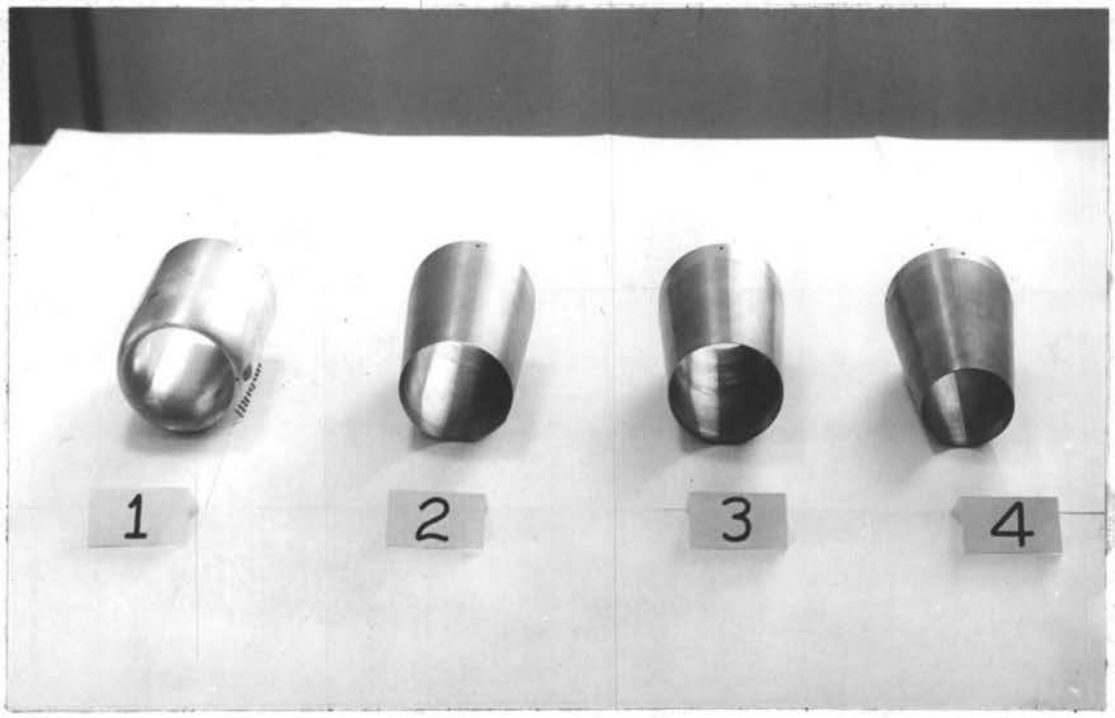

Figure 6

Four Basic Inlets

Inlet 4. This inlet had sharp lips and a constant diameter internal contour. The design purpose of this inlet was to serve as a base for the determination of the effect of contraction ratio.

The basic inlets, 2, 3 and 4, were altered so as to determine the effect of blowing or sucking air through the walls of the inlet. In order to blow through the walls, a V shaped slot, shown in figure 7, was cut in the immediate region of the lips. Air was allowed to flow through this slot. The inlets thus formed are numbered 5, 6, and 7, respectively.

Figure 7

Inlet with Slot Cut Near the Lip

The slots used for blowing through the walls were then covered by metal strips and tubes attached at intervals of 60° around the periphery of the inlets. Air was then sucked through these tubes. The resulting inlets, as shown in figure 8, were numbered 8, 9, and 10.

Figure 8

Inlet with Alteration
To Suck Air Through Wall

The remainder of the duct was designed so as to provide good subsonic diffusion of the air. The entire model is as shown in figure 9.

The apparatus, showing the duct in place for testing the inlets, is shown in figure 10. The intake to a centrifugal compressor was used to draw the air through the duct. This compressor was powered by a 7-1/2 horsepower Varibelt drive. The apparatus for sucking the air through the walls of the inlet is shown in figure 11.

In order to gain some concept of the flow into the sharp edged inlets, a splitter plate was placed in inlets 2, 3, and 4. A mixture of kerosene and lampblack was sprayed onto these plates and the resulting flow pattern then photographed. The apparatus for doing this is shown in figure 12.

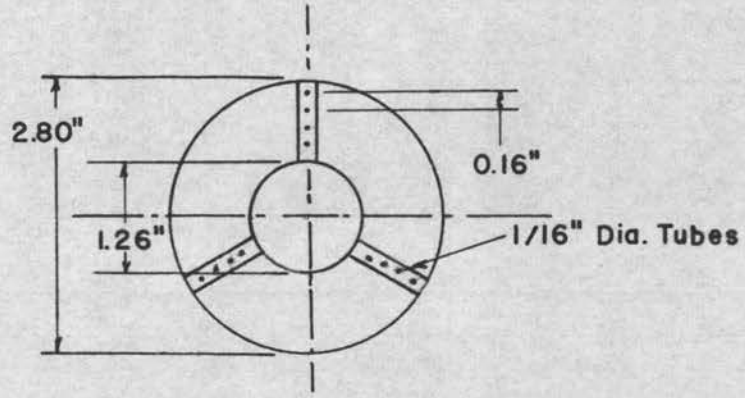

Face View of Compressor Entrance
(Station C)

Station	Outside Dia.	Inside Dia.
0	2.5"	2.5"
1	3.0"	2.0"
C	3.8"	2.8"
D	3.8"	2.8"
E	7.0"	7.0"

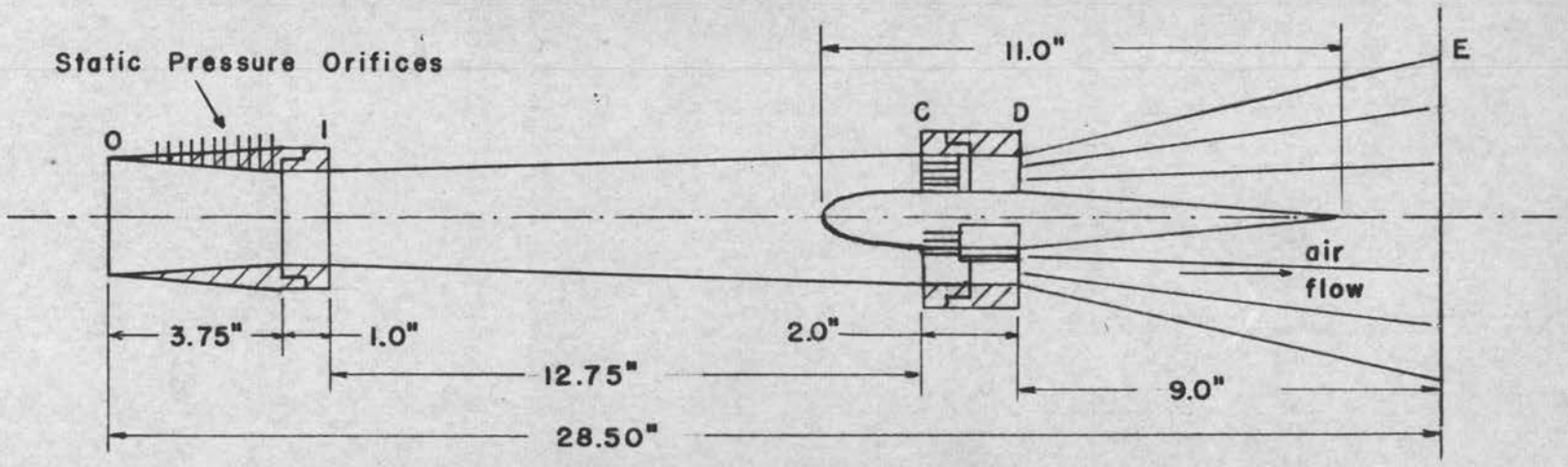

FIG. 9 OVERALL DETAILS OF MODEL DESIGN

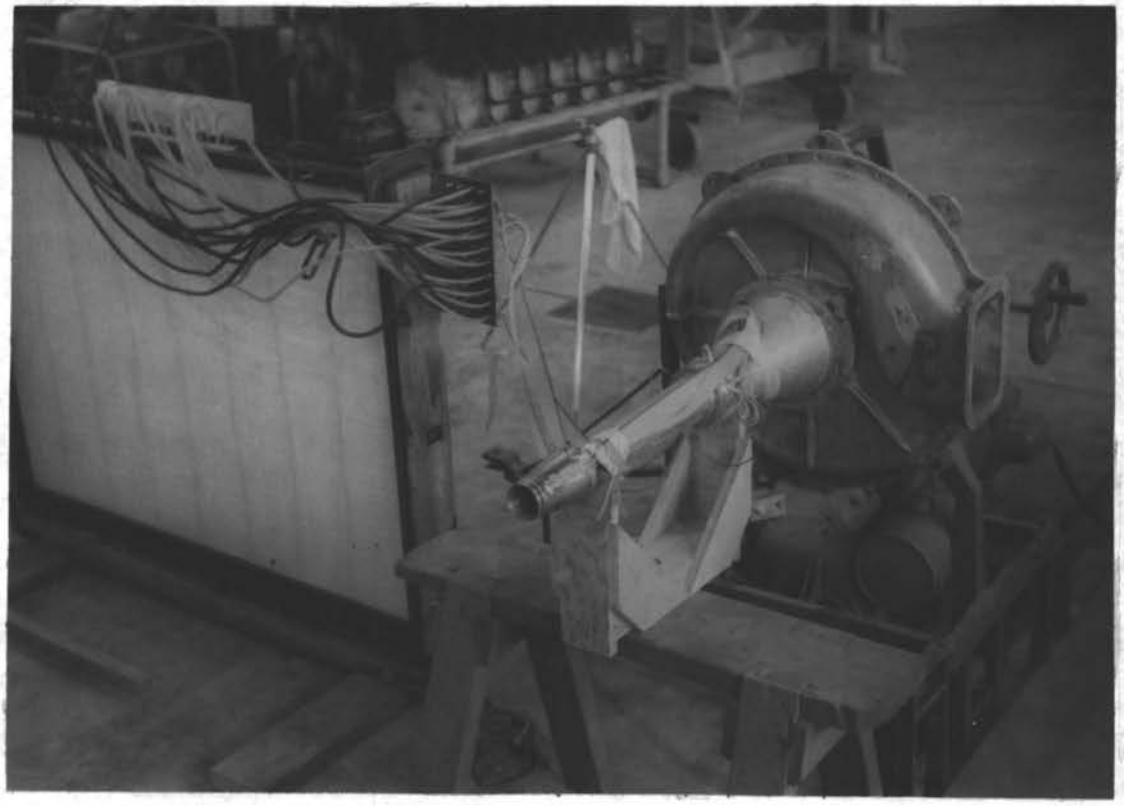

Figure 10

View of Entire Test Apparatus

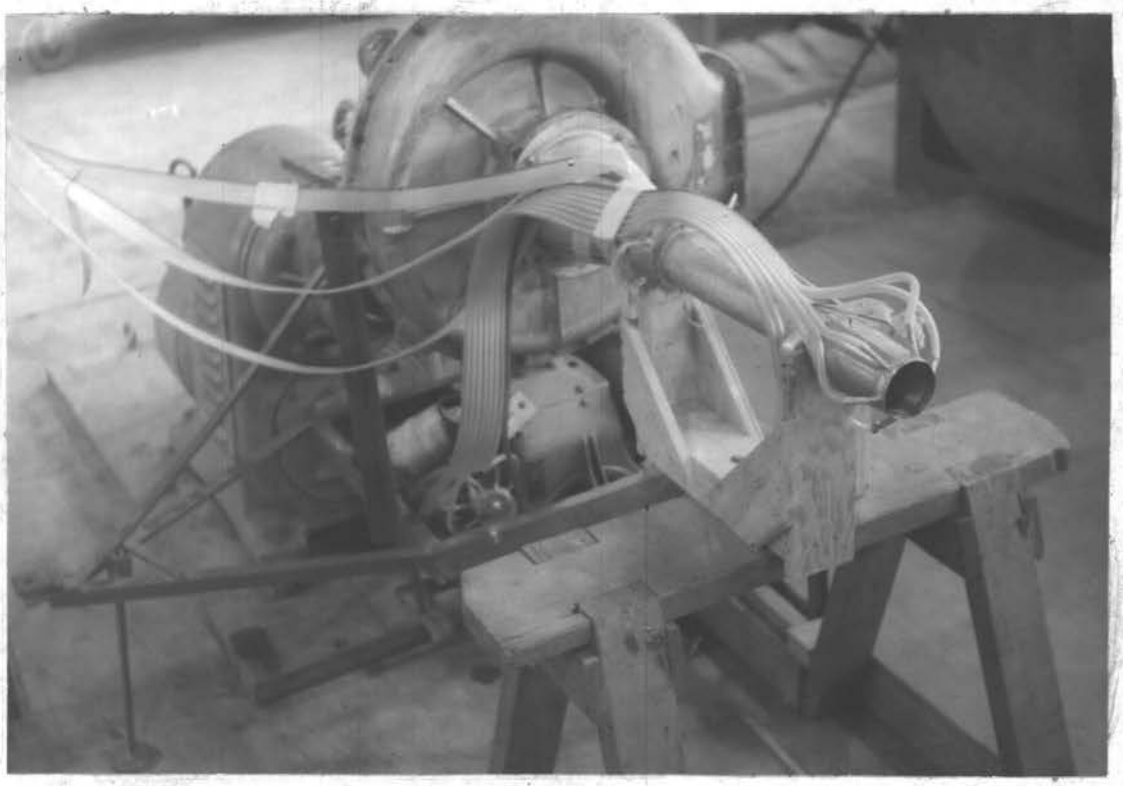

Figure 11

Apparatus for Drawing Air Through Wall of Inlet

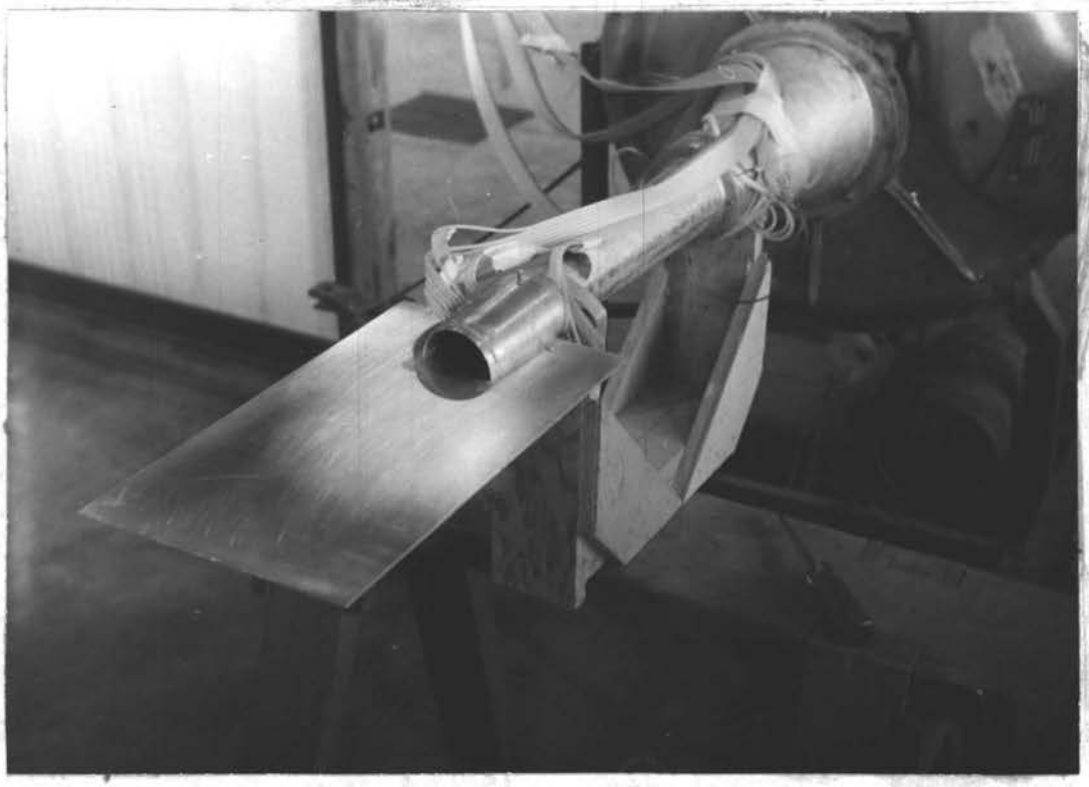

Figure 12

Apparatus for Kerosene and Lampblack Method
of Flow Visualization

Instrumentation

Each of the inlets had eleven static pressure orifices along the wall of the inlet. These began one inch aft of station 0, and were spaced at one-quarter inch intervals along the wall. These orifices are shown for inlet 2 in figure 9.

At the simulated compressor entrance, station C, twelve total pressure tubes were oriented as shown in figure 9. Three static pressure orifices were also placed at this station.

A multiple manometer board was used to measure all of the pressures at one time. A photograph was taken of the manometer board for each point in the tests. These photographs were read to an accuracy of 1/10 inch of mercury.

Tests

Four series of tests were run. In each series of tests, the static pressure distribution along the wall of the inlet was determined as well as the total pressure ratio. The first series consisted of testing the four basic inlets 1, 2, 3, and 4. The second series consisted of testing inlets 5, 6, and 7. In this series, air was blown through the walls of the inlet. No attempt to establish directional control upon this air was made. Inlets 8, 9, and 10 were tested in the third and fourth series. In the third series air was sucked through the walls of the inlet, while in the fourth series, no air was drawn off.

RESULTS AND DISCUSSION

Properties of the Internal Flow

The entire problem of the static performance of inlets arises from the inability of the air flow to experience an abrupt change of direction without separating from the walls. In order to get some concept of the nature of this separation of the air flow into the inlets, tuft studies were made.

The tuft studies indicated that for inlet 1, the flow was only slightly separated from the walls of the inlet. The study for the sharp edged inlets indicated that the air flow separated from the walls of the inlet in the immediate region of the lips.

This separation of the flow from the walls of the inlet is further evidenced upon examination of the results of the kerosene and lamp-black method of flow visualization shown in figures 13 a, b, and c.

The flow pattern for inlet 2 is shown in figure 13 a. The air enters the duct from all directions. In travelling around the sharp lip, the flow separates from the wall of the inlet, but also re-attaches aft of the lips. The flow then separates and accelerates in the converging channel of the inlet.

The flow for inlet 3 follows the same general pattern as for inlet 2. This flow is presented in figure 13 b. The point of reattachment is farther forward and the separation after that point is not as great as in the case of inlet 2.

The flow for inlet 4 is shown on figure 13 c. The flow into this inlet separates a much greater amount than the flow into

Figure 13 a

Flow Pattern of Air into Inlet 2, $M_c = 0.37$

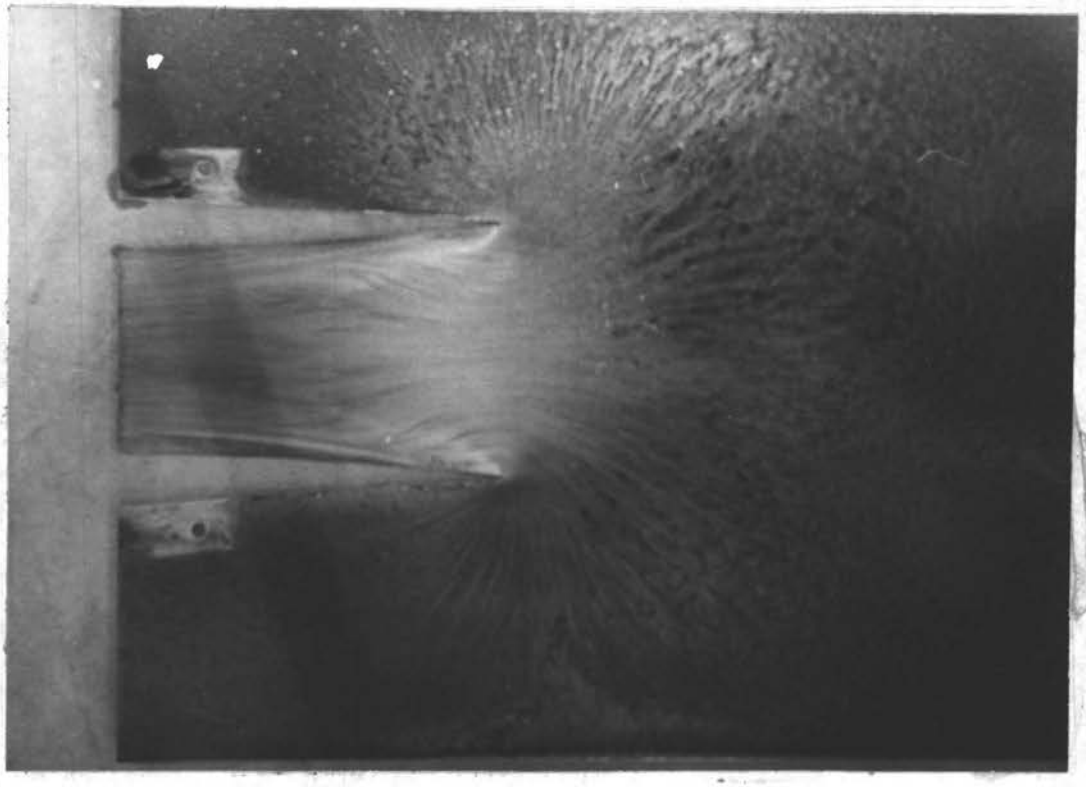

Figure 13 b

Flow Pattern of Air into Inlet 3, $M_c = 0.35$

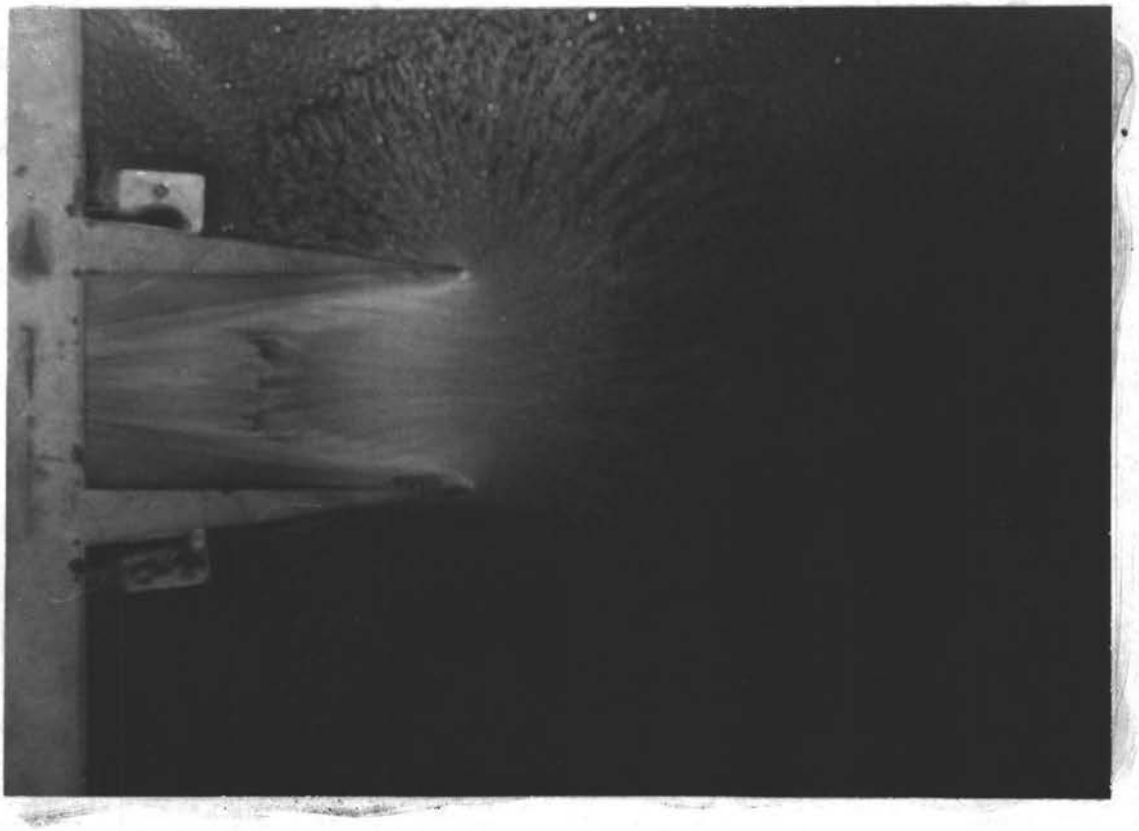

Figure 13 c

Flow Pattern of Air into Inlet 4, $M_c = 0.29$

inlets 2 and 3. The flow never became fully reattached to the walls of the inlet.

The foregoing observations can be seen upon study of the static pressure distributions presented in figures 14 a, b, c, and d. The static pressure distributions for the four basic inlets are shown in figure 14 a. These distributions are for the maximum Mach number reached with each inlet.

The tuft studies are verified in the case of inlet 1. The static pressure ratio remained very nearly constant for the entire length of the inlet, indicating little or no region of separation near the lips.

In the case of inlets 2 and 3, the static pressure ratio was low in the forward region, rose and then decreased along the length of the inlet. This indicated that the flow was separated in the region of the lips and became fully reattached at the point of maximum static pressure ratio. It is significant to note that the flow became fully reattached nearer the lips for inlet 3 than for inlet 2.

The static pressure distribution for inlet 4 indicated there was a large region of separated flow near the lips. The flow never became fully reattached along the entire length of the inlet.

The remaining three curves, 14 b, c, and d, are for the second, third and fourth series of tests respectively. It will be recalled that air was blown through the walls of the inlets for the second series, while air was drawn through the walls for the third series. The fourth series of tests used the same inlets as the third, but no air was drawn through the walls. The general pattern for each of the inlets is similar to the corresponding inlet for the first series of

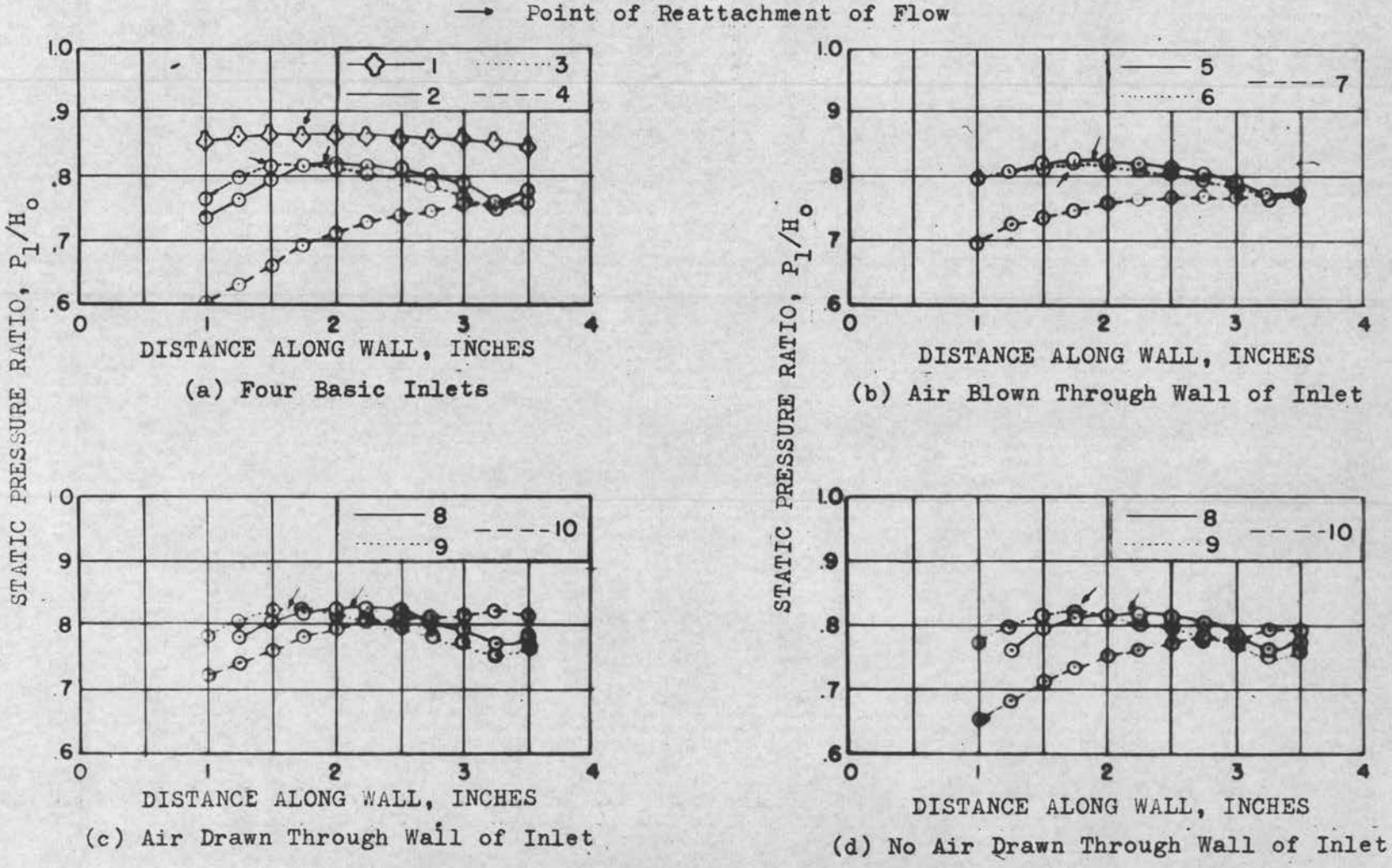

FIG. 14 STATIC PRESSURE DISTRIBUTION ALONG THE WALL OF EACH INLET

tests. The point of reattachment has moved rearward in all cases, but this point is still farther forward for the curved wall inlet than for the straight wall inlet.

During the actual course of the testing, an indication of the nature of the flow could be gained from the pattern of the pressure tubes on the multiple manometer board. Photographs of the manometer boards for one run of the four basic inlets are shown in figure 15. The tubes are, numbering from the left, arranged as follows: tube 1, atmospheric pressure; tubes 2-13, total pressure at the simulated compressor entrance; tube 14, static pressure at the compressor entrance; tube 15, atmospheric pressure; and tubes 16-26, static pressures along the wall.

The pattern for these tubes corresponds roughly to the inverted static pressure distribution curves of figure 14. The high tubes at the beginning of the static tubes indicate the flow was separated from the wall. The lowest reading tube indicates the point of reattachment of the flow.

Total Pressure and Mass Flow Ratios

As the flow travelled around the lips and separated from the walls, some of the total energy of the flow was lost. This loss of total energy was indicated throughout the test by the high negative pressure readings by the total pressure tubes in figure 15. For the four basic inlets used in the first series of tests, the total pressure was found to vary over the face of the compressor entrance. This variation is shown in figure 16.

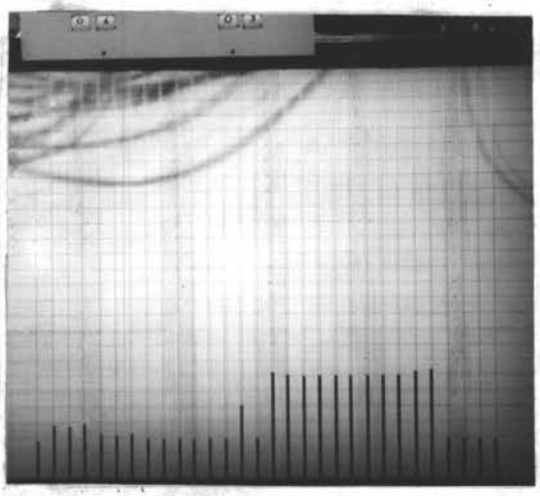

(a) Inlet 1, $M_c = 0.30$

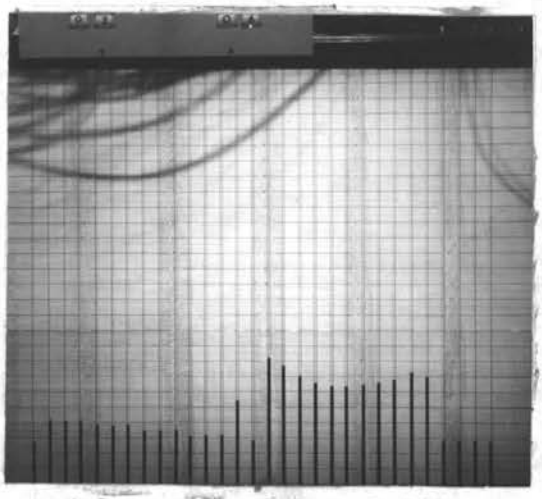

(b) Inlet 2, $M_c = 0.305$

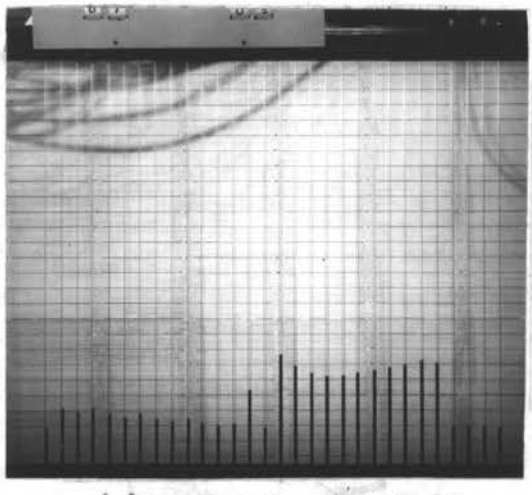

(c) Inlet 3, $M_c = 0.30$

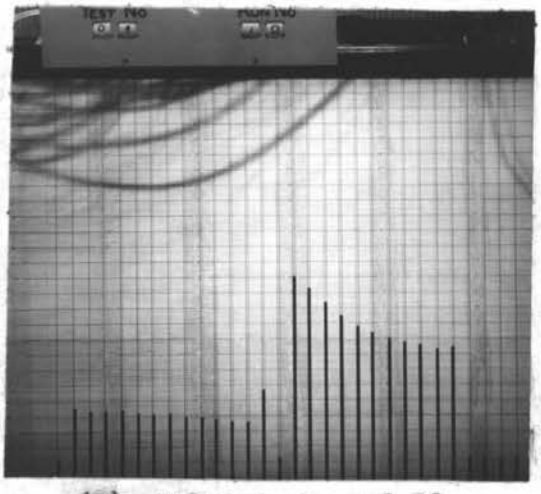

(d) Inlet 4, $M_c = 0.30$

Figure 15

Manometer Board Pattern for Four Basic Inlets

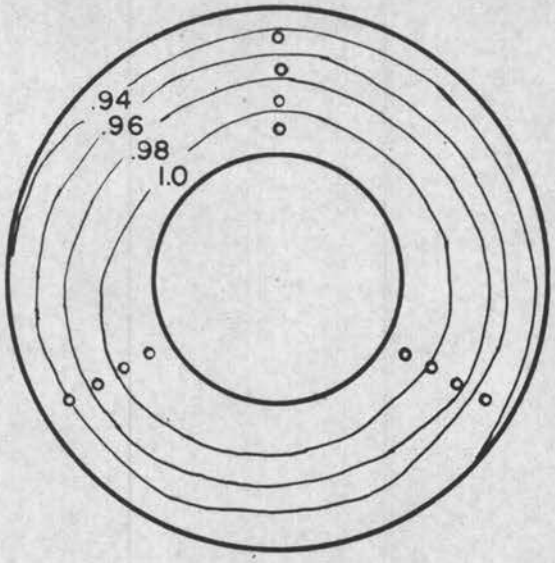

INLET 1

M_c=0.42

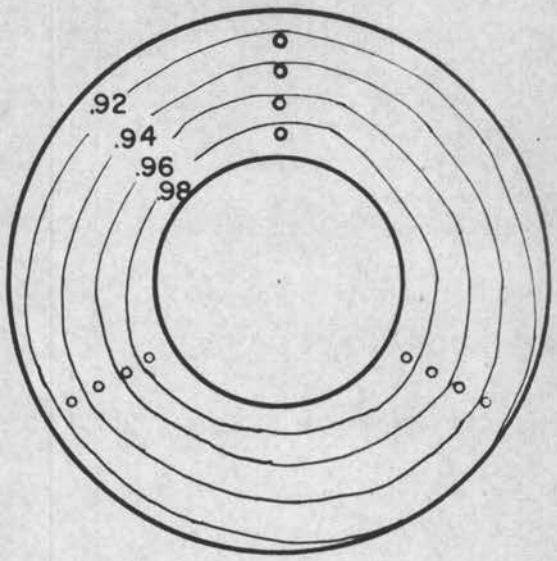

INLET 2

M_c=0.375

Contour Lines Are For Constant Total Pressure Ratio

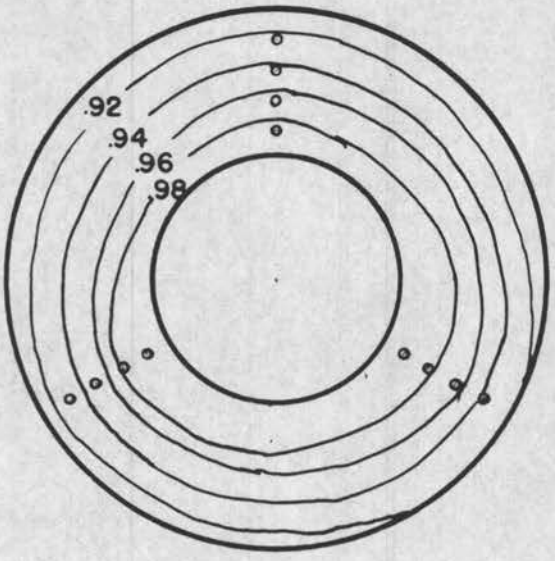

INLET 3

M_c=0.395

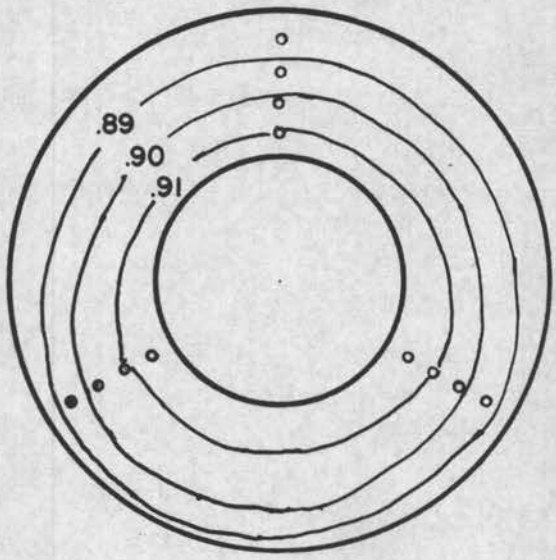

INLET 4

M_c=0.30

FIG. 16 TOTAL PRESSURE MAPS AT THE FACE OF THE COMPRESSOR

The total pressure variation followed the same general pattern for all of the inlets. The greatest loss in total pressure was experienced near the walls of the duct. This indicates that either due to friction along the walls, or due to losses associated with the lips, total energy has been lost in the inlet. Since the friction factors would be dependent only on the length, which was held constant, the difference in the individual inlets would be due to lip losses.

The ability of the inlet to recover the total pressure at the compressor entrance is one measure of the efficiency of the inlet. The total pressure ratios, H_c/H_o, for all of the inlets tested are shown as functions of compressor entrance Mach number, M_c, in figure 17 a, b, c, and d.

The total pressure ratios for the first series of tests are shown in figure 17 a. The total pressure ratio for inlet 1 is nearly isentropic over the entire range of compressor entrance Mach number. The losses that occurred in this inlet are probably associated with the friction losses along the walls of the duct.

The total pressure ratio for the sharp edged inlet with no contraction ratio, inlet 4, deviates largely from the isentropic value. Comparison of the performance of this inlet with the sharp edged inlet with contraction ratio indicates that the static performance can be largely improved by the use of the contraction ratio. The improvement is of the order of 7% at an $M_c = 0.30$.

Comparison of the total pressure ratios for the straight and curved wall inlets, 2 and 3, with the same contraction, indicated that the curved wall inlet gave a slightly higher total pressure ratio.

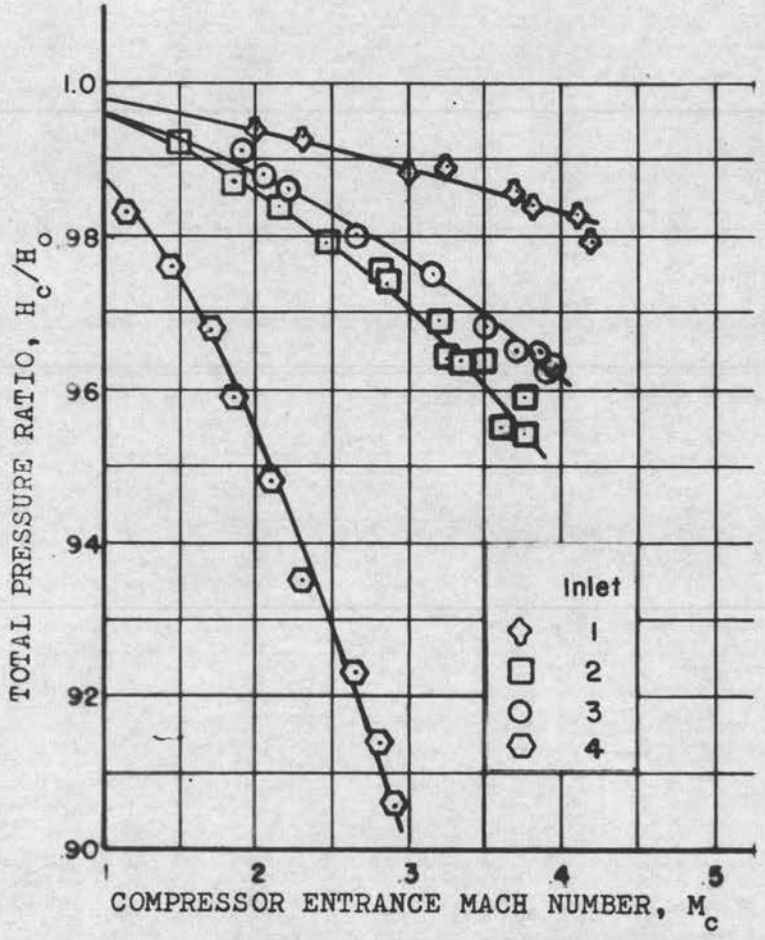

(a) Four Basic Inlets

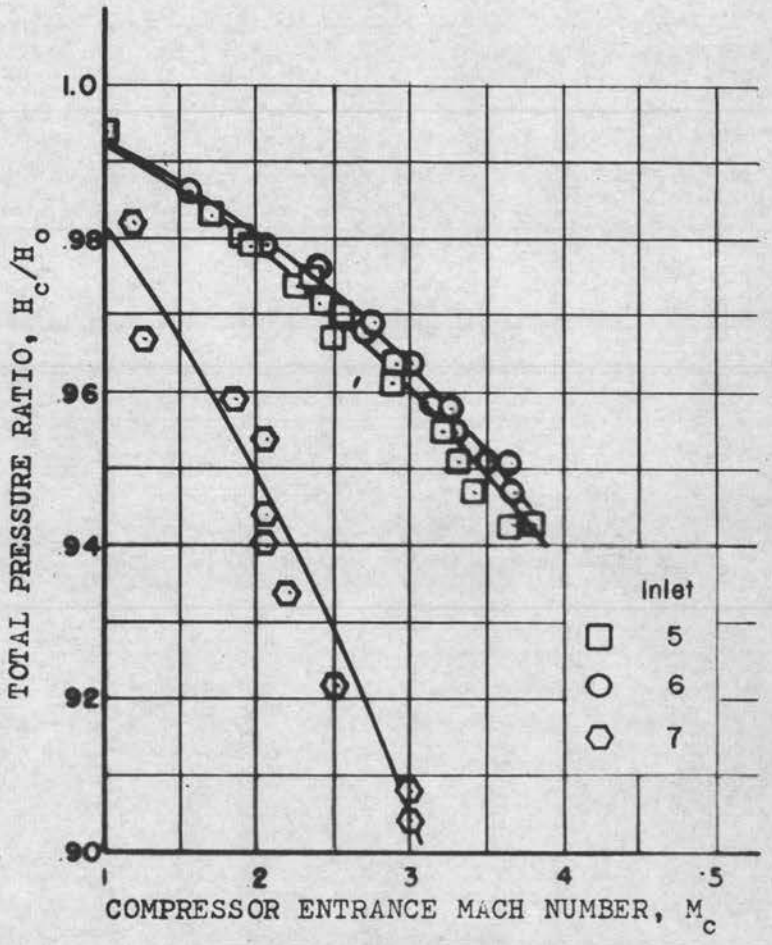

(b) Air Blown Through Wall of Inlet

FIG. 17 THE VARIATION OF TOTAL PRESSURE RATIO VERSUS COMPRESSOR INLET MACH NUMBER

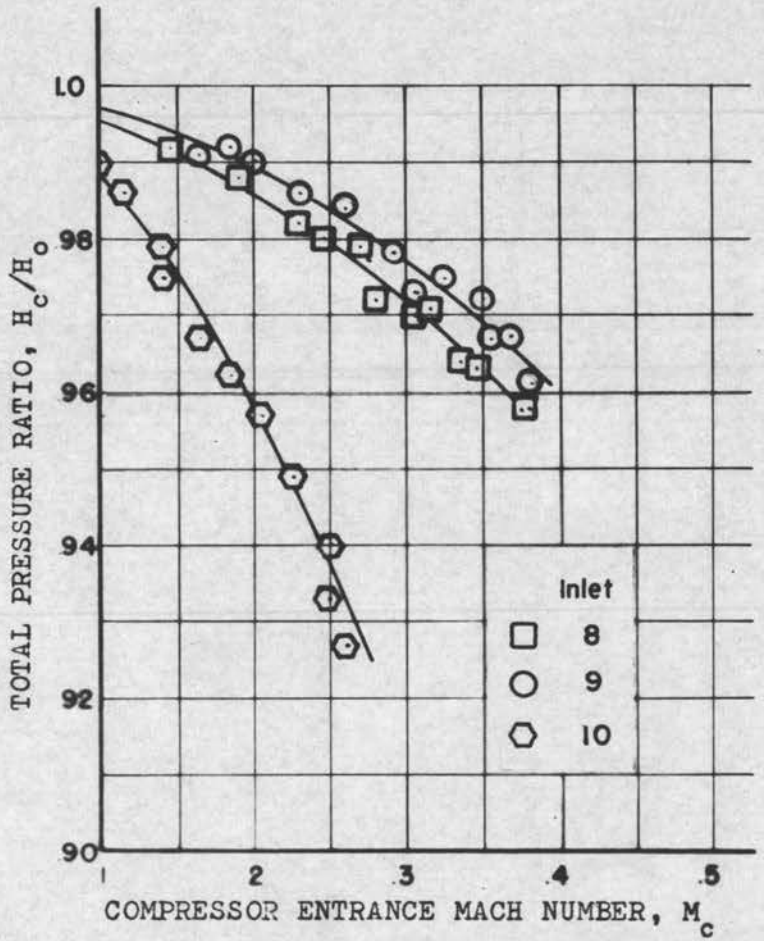

(c) Air Drawn Through Wall of Inlet

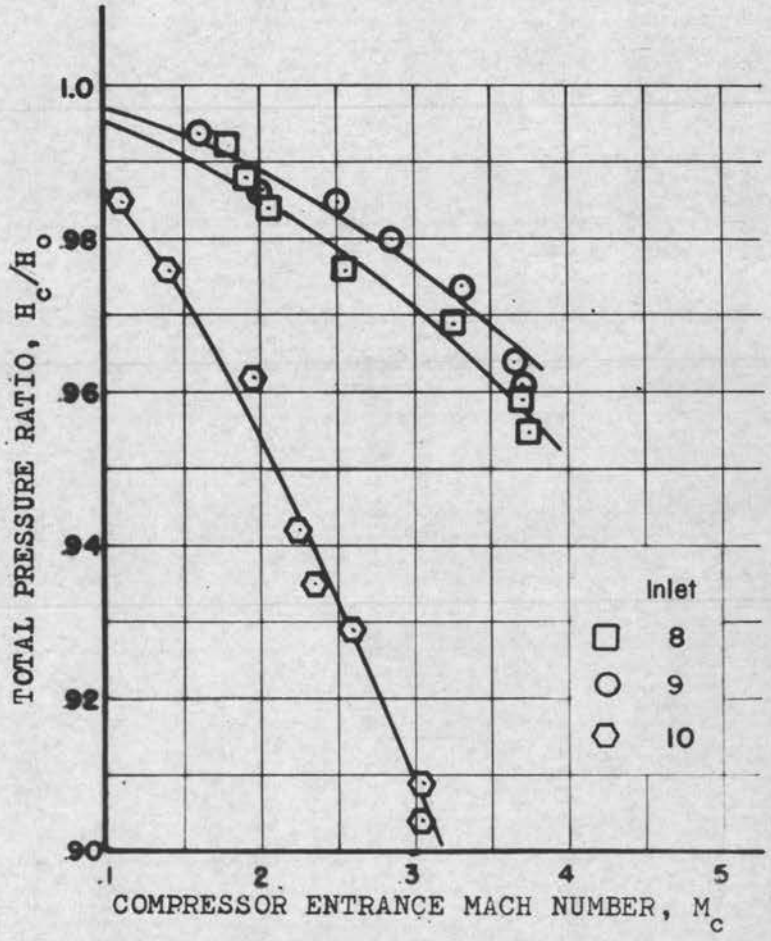

(d) No Air Drawn Through Wall of Inlet

FIG. 17 THE VARIATION OF TOTAL PRESSURE RATIO VERSUS COMPRESSOR INLET MACH NUMBER

This rise is of the order of 0.7% for a $M_c = 0.3$. The total pressure ratio for inlet 3 compares favorably with that for inlet 1. The difference being that inlet 3 had a 1% lower total pressure at $M_c = 0.30$.

The difference in the total pressure ratios of these inlets seems to be directly associated with the static pressure distributions of the inlets. The improvement of inlet 2 over inlet 4 can be associated with the fact that the flow reattached. The improvement of inlet 3 over inlet 2 can be attributed to the more forward reattachment of the flow for inlet 3. Since inlet 1 had no separation, the moving forward of the point of reattachment of the flow tends to make the inlet more nearly isentropic.

The results of the second series of tests, inlets 5, 6, and 7, are given in figure 17 b. The effect of blowing air into the inlets is to reduce the total pressure ratio of inlets 5 and 6. The effect upon inlet 7 was negligible.

The lowering of the total pressure ratios for these inlets is due to the fact that the airflow through the slots was perpendicular to the airflow inside of the inlet. The kinetic energy of the air flowing through the slots was less than that of the airflow in the inlet; therefore, some of the kinetic energy of the airflow in the inlet was lost in accelerating the air blown through the slots. A loss in kinetic energy means the total energy available would be less, or that there would be a loss in the total pressure that could be recovered.

Any air that would be blown into the inlet could be thought of as composed of two components, one parallel to the airflow in the inlet, and one perpendicular to it. The kinetic energy of the

component parallel to the airflow in the inlet would have to be greater than that of the airflow in order to improve the total pressure ratio. This means that the air would have to be blown into the inlets at high pressure and through slots slanted rearward.

The total pressure ratios of inlets 5 and 6 were more nearly equal than they were for inlets 2 and 3. This can also be attributed to the points of reattachment of flow for the inlets. The air flowing through the slots has moved the points of reattachment rearward and closer together, thus making the total pressure ratios lower and more nearly the same.

The total pressure ratios for inlets 8, 9, and 10, are shown in figure 17 c and d. The effect of sucking air through the walls of the inlet is shown in figure 17 c. The total pressure ratios of figure 17 c must be compared with those of figure 17 d (no air drawn out), in order to allow for the effect of the apparatus used to draw the air through the walls of the inlet. There is some slight indication that the total pressure ratio was improved when air was drawn from the inlets, but this difference was not enough to allow any conclusion. The lack of any conclusive results for this test probably due to the fact that the quantity of air drawn from the inlets was too small.

The mass flow ratios m_c/m_* are shown as a function of compressor entrance Mach number M_c, in figures 18 a, b, c, and d. The mass flow at the similated compressor entrance was found to be proportional to the total pressure ratio at that particular M_c. The mass flow ratio, m_*, is the mass flow required to give a Mach number of unity at the point of minimum area. The derivation of the equations used in

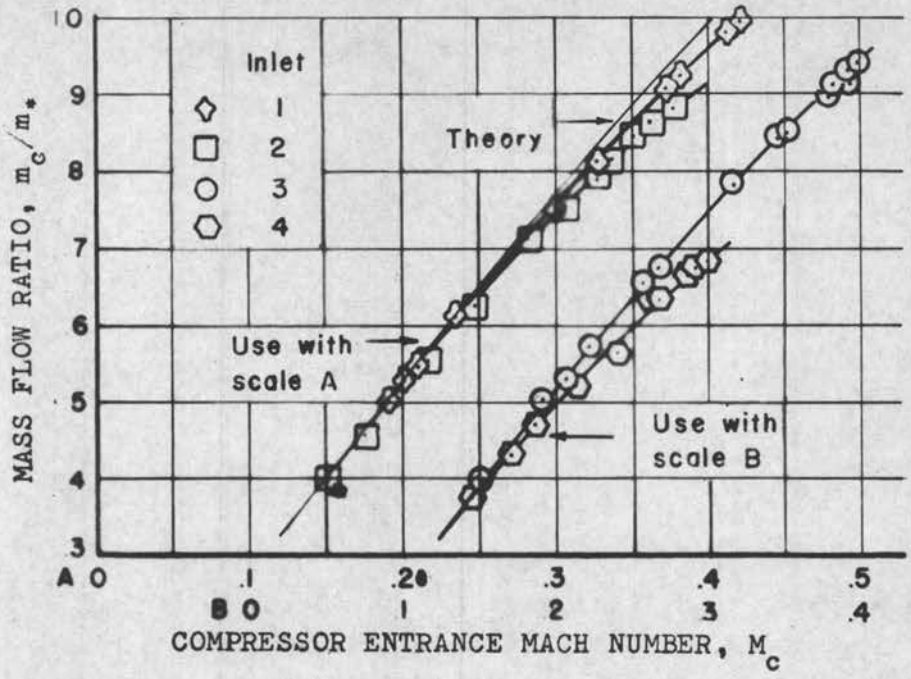

(a) Four Basic Inlets

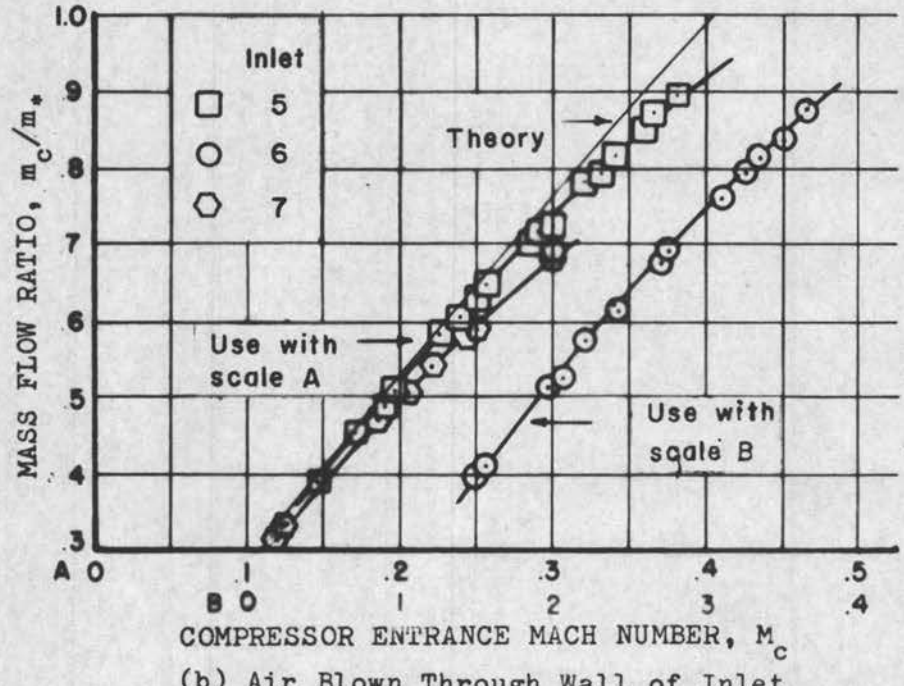

(b) Air Blown Through Wall of Inlet

FIG. 18 THE VARIATION OF MASS FLOW RATIO VERSUS COMPRESSOR INLET MACH NUMBER

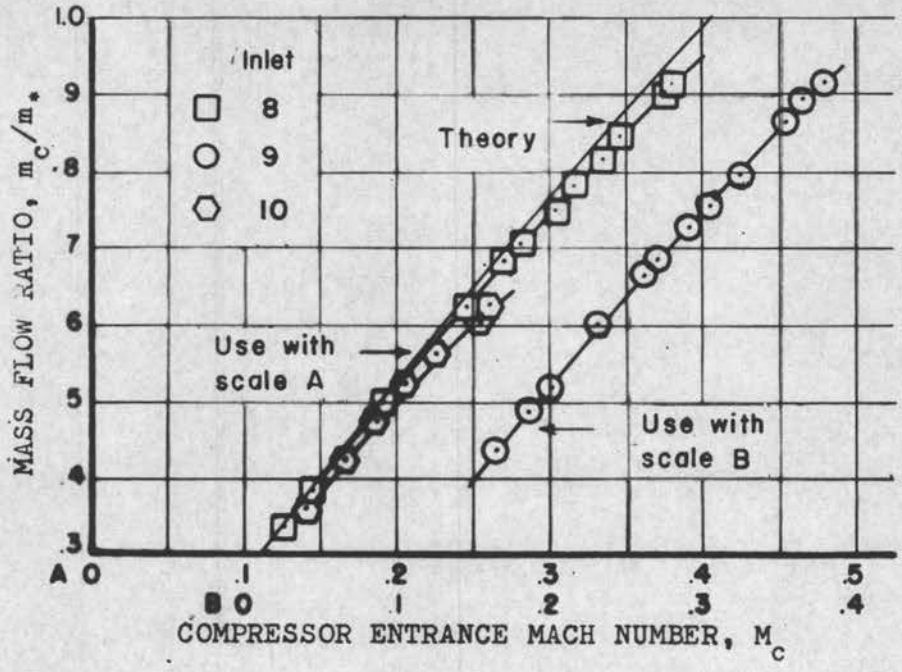

(c) Air Drawn Through Wall of Inlet

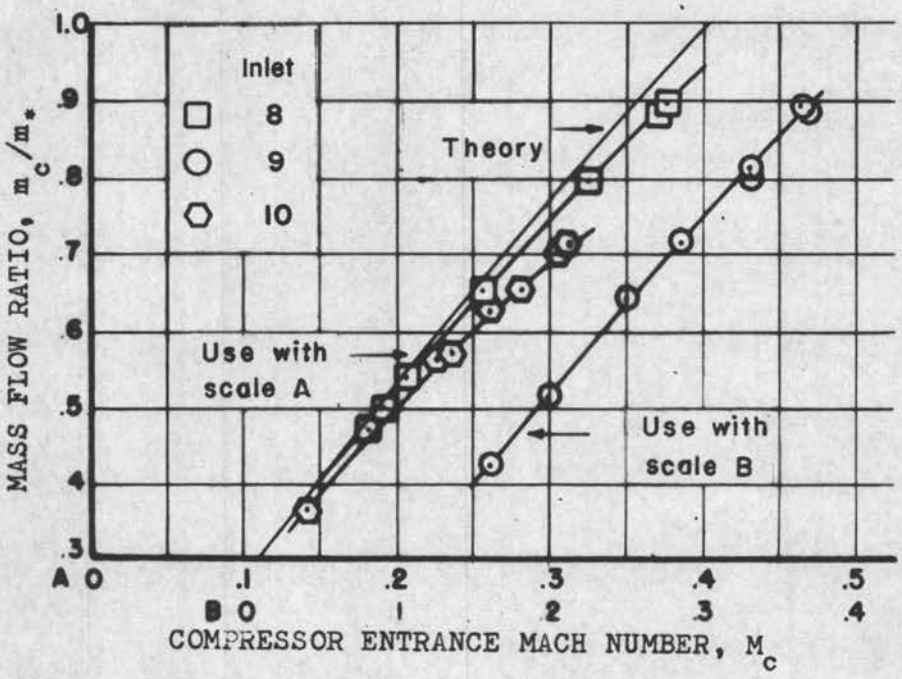

(d) No Air Drawn Through Wall of Inlet

FIG. 18 THE VARIATION OF MASS FLOW RATIO VERSUS COMPRESSOR INLET MACH NUMBER

computing this ratio can be found in the appendix. The resulting equation that was used in finding the mass flow ratio was:

$$\frac{m_c}{m} = \frac{(\rho V)_{ci}}{(\rho V)_*} \frac{H_c}{H_o} \frac{A_c}{A}$$

where $(\rho V)_{ci}$ is the isentropic mass flow per unit area at the compressor entrance.

The mass flow ratios for the first series of inlets are shown in figure 18 a. The elliptical lipped inlet, 1, gave very nearly theoretical or isentropic mass flow ratio for the entire range of M_c. Of the sharp edged inlets, inlet 3 had the most nearly theoretical mass flow ratio with inlets 2 and 4 following in order.

The mass flow of inlets 5, 6, and 7, are shown in figure 17 b. The mass flow ratios for these inlets are slightly lower than those for 2, 3, and 4, respectively, as would be expected from the relationship of the total pressure ratios for the two series. Here again, the curved wall inlet, 6, had the best performance, with 5 and 7 following in order.

The mass flow ratios for inlets 8, 9, and 10, are shown in figures 17 c and d. The mass flow ratio for each inlet with air being drawn out is essentially the same as when no air is drawn out. A complete discussion of the factors affecting the mass flow ratios would be repetitious of the discussion for the total pressure ratios.

CONCLUSION

The immediate conclusions that can be made from the results of the tests conducted for this investigation are:

1. The performance of sharp edged inlets having contraction ratio is significantly better than the performance of the inlet having no contraction ratio.
2. For inlets having the same contraction ratio, the performance of the inlet having a slight curvature of its internal walls was better than the inlet having straight internal walls. The inlet with curved walls gave total pressure ratios that were fairly close to those for an inlet that had thick elliptical lips. The thick lipped inlet was known to have near isentropic static performance.
3. The performance of all the sharp edged inlets was decreased by flowing through the walls of the inlets. This air entered the inlet perpendicular to the axis of symmetry.
4. In light of the performance of the curved wall inlet, it is felt that the use of various types of boundary layer control would be unnecessary.

The results of this investigation are quite incomplete and can only be used to give an indication of the value of the design parameters used. The equipment that was available was not sufficient to obtain the full range of mass flow ratios needed to give maximum operating conditions. Much work needs yet to be done in optimizing the amount of contraction ratio and internal wall curvature.

A correlation of these design parameters upon the supersonic performance would then have to be established.

BIBLIOGRAPHY

1. Blackaby, James R., and Earl C. Watson. An experimental investigation at low speeds of the effects of lip shape on the drag and total pressure recovery of a nose inlet in a body of revolution. Washington, National advisory committee for aeronautics, 1954. 48p. (NACA technical note 3170)

2. Dailey, C. L., and F. C. Wood. Computation curves for compressible fluid problems. New York, John Wiley and sons, inc., 1949. 33p.

3. Durham, Franklin P. Aircraft jet powerplants. 2nd ed. New York, Prentice-Hall, inc., 1953. 326p.

4. Fradenburgh, E. A., and D. D. Wyatt. Theoretical performance of sharp lips at subsonic speeds. Washington, National advisory committee for aeronautics, 1954. 8p. (NACA report 1193)

5. Kuchemann, Dietrich, and Johanna Weber. Aerodynamics of propulsion. New York, McGraw-Hill book company, inc. 1953. 340p.

6. National advisory committee for aeronautics. Equations, tables and charts for compressible flow. Washington, 1953. 68p. (NACA report 1135)

7. Sheddon, J. Air intakes for aircraft gas turbines. Journal of the royal aeronautical society. 56:749-787. Oct. 1952.

APPENDIX

TABLE I

COORDINATES FOR INTERNAL WALLS OF INLET 3

STATION	INTERNAL DIAMETER
0	2.50
1/4	2.438
1/2	2.386
3/4	2.340
1	2.296
1 1/4	2.262
1 1/2	2.224
1 3/4	2.192
2	2.146
2 1/4	2.126
2 1/2	2.096
2 3/4	2.066
3	2.044
3 1/4	2.026
3 1/2	2.010
3 3/4	2.00

DERIVATION OF MASS FLOW EQUATIONS

The continuity equation at any point is

$$m = \rho VA$$

$$\frac{m}{A} = \rho V$$

$$\frac{m}{A} = \rho \frac{V}{a} a = \frac{\rho_o \rho}{\rho_o} Ma$$

but $\frac{\rho}{\rho_o} = (1 + \frac{\gamma-1}{2} M^2)^{-\frac{1}{\gamma-1}}$, thus

$$\frac{m}{A} = \rho_o (1 + \frac{\gamma-1}{2} M^2)^{-\frac{1}{\gamma-1}} Ma$$

and the equation of state give $\rho_o = \frac{H_o}{Rt_o}$, thus

$$\frac{m}{A} = \frac{H_o}{Rt_o} M a (1 + \frac{\gamma-1}{2} M^2)^{-\frac{1}{\gamma-1}}$$

$$\frac{m}{A} = \frac{H_o}{Rt_o} M a \frac{\sqrt{R}}{\sqrt{R}} \frac{\sqrt{t_o}}{\sqrt{t_o}} \frac{\sqrt{\gamma}}{\sqrt{\gamma}} (1 + \frac{\gamma-1}{2} M^2)^{-\frac{1}{\gamma-1}}$$

$$\frac{m}{A} = \frac{H_o}{\sqrt{\gamma R t_o}} M a \sqrt{\frac{\gamma}{Rt_o}} (1 + \frac{\gamma-1}{2} M^2)^{-\frac{1}{\gamma-1}}$$

but $\sqrt{\gamma R T_o} = a_o$ and $\frac{a}{a_o} = (1 + \frac{\gamma-1}{2} M^2)^{-\frac{1}{2}}$, thus

$$\frac{m}{A} = \frac{H_o M}{\sqrt{t_o}} \sqrt{\frac{\gamma}{R}} (1 + \frac{\gamma-1}{2} M^2)^{-\frac{\gamma+1}{2(\gamma-1)}}$$

If this equation is applied to the duct,

$$\frac{m_c}{A_c} = \frac{H_c M_c}{\sqrt{t_c}} \sqrt{\frac{\gamma}{R}} \left(1 + \frac{\gamma-1}{2} M_c^2\right)^{-\frac{(\gamma+1)}{2(\gamma-1)}}$$

and since $\frac{H_c}{H_o}$ is known and $t_c = t_o$

$$\frac{m_c}{A_c} = \frac{H_c}{H_o} \left[\frac{H_o M_c}{\sqrt{t_o}} \left(1 + \frac{\gamma-1}{2} M_c^2\right)^{-\frac{(\gamma+1)}{2(\gamma-1)}} \right]$$

The quantity in brackets is the isentropic mass flow per unit area at the compressor entrance, thus

$$\frac{m_c}{A_c} = \frac{H_c}{H_o} (\rho V)_{ci}$$

Thus the mass flow ratio for the inlets would be

$$\frac{m_c}{m_*} = \frac{H_c}{H_o} \frac{A_c}{A_*} \frac{(\rho V)_{ci}}{(\rho V)_*}$$

Curves are available for m_{ci}, and m_* is constant for any given area, thus these computations are easily made.